



Enhanced measurement of high aspect ratio surfaces by applied sensor tilting

Alexander Schuler¹, Albert Weckenmann¹, Tino Hausotte²

¹ Friedrich-Alexander-Universität Erlangen-Nürnberg, Chair Quality Management and Manufacturing Metrology (QFM), Naegelsbachstrasse 25, 91052 Erlangen, GERMANY

² Friedrich-Alexander-Universität Erlangen-Nürnberg, Institute of Manufacturing Metrology (FMT), Naegelsbachstrasse 25, 91052 Erlangen, GERMANY

ABSTRACT

During tactile surface measurements the contact point between probing tip and surface varies depending on the local surface angle. To reduce the resulting measurement deviation on high slopes a probing principle is investigated that applies a dynamic surface dependent sensor tilt. This probing process and the logics for the angle determination have been evaluated by simulation. A test stand based on a nanometer coordinate measuring machine is developed and fitted with a rotation kinematic based on stacked rotary axes. Systematic positioning deviations of the kinematic are reduced by a compensation field. The test stand has been completed and results are presented.

Section: RESEARCH PAPER

Keywords: Profilometry; servo system; uncertainty; simulation

Citation: Alexander Schuler, Albert Weckenmann, Tino Hausotte, Enhanced measurement of high aspect ratio surfaces by applied sensor tilting, Acta IMEKO, vol. 3, no. 3, article 6, September 2014, identifier: IMEKO-ACTA-03 (2014)-03-06

Editor: Paolo Carbone, University of Perugia

Received June 4th, 2013; **In final form** July 31th, 2014; **Published** September 2014

Copyright: © 2014 IMEKO. This is an open-access article distributed under the terms of the Creative Commons Attribution 3.0 License, which permits unrestricted use, distribution, and reproduction in any medium, provided the original author and source are credited

Funding: This work was supported by the German Research Foundation (DFG), Germany

Corresponding author: Alexander Schuler, e-mail: alexander.schuler@fau.de

1. INTRODUCTION

For tactile surface measurements the surface topography is superimposed with the shape of the probing element and a morphological filtering is performed [1]. The actual contact point varies depending on the local surface slope and the tip's form. In contrast to 3D coordinate measuring machines with 3D force sensors, tactile scanning systems like profilometers or AFMs (atomic force microscope) use a fixed probing force direction, assuming a probing point at the front of the applied tip [2], [3]. Without its actual knowledge large deviations occur on steep surfaces as the expected reference contact point is left. The resulting deviation can be compensated arithmetically to a certain degree [4], but when the probing point leaves the spherical front, the recorded trace can no longer be unambiguously reconstructed, practically limiting the application range. Usual tactile tips feature a conical or pyramidal base with a very small apex radius, limited by mechanical stability. For profilometers the base angle is usually up to 90 ° with apex radii up to 2 µm. Figure 1 (left) shows the surface reconstruction when the front of the sensor tip is

assumed as a probing point. During flank contacts the deviation increases significantly and especially occurs during the measurement of workpieces with high slopes and high aspect ratios as e.g. cutting tools, freeform lenses or microstructures like micro lens arrays. This problem restricts the application of tactile surface probing to surfaces with limited curvature [5]. A probing principle is investigated to lift this restriction. An orthogonal orientation to the surface is kept during the measurement by using a dynamic surface slope dependent tip rotation, displayed in Figure 1 (right). Research has shown that the deviation on steep flanks can be reduced by using angled probes. But this leads to a higher measurement deviation for the rest of the sample [6]. With repeated measurements under different angles and the application of sensor data fusion the whole surface can be acquired. Yet this requires lots of time and introduces additional contributions to the measurement uncertainty [7], [8], [9]. Instead by using sensor tilting during measurement both disadvantages are avoided. To reach this goal, research has been carried out [10]. In a first step the contact behaviour and the tilting process was implemented into a simulation environment (section 2). This allowed an early

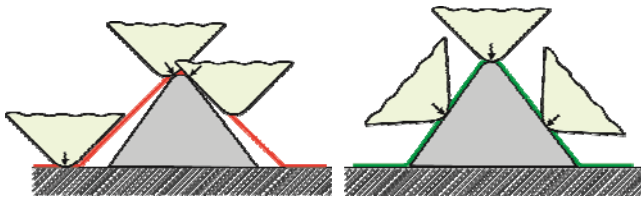


Figure 1. Left: No compensation; Right: With compensation.

evaluation of the measurement deviation reduction and the development of algorithms to allocate a tilt angle of the tip to a surface point. With the simulation results the kinematic chain was chosen (section 3), sensor and calibration artefacts were selected (section 4) and preliminary tests (section 5) were conducted. Afterwards the prototype setup was finished (section 6) and measurement results were acquired (section 7).

2. EVALUATION BY SIMULATION

The working principle of the simulator is based on collision checking between a tip model and a discretized surface model. A simplified 2D representation is selected to reduce the complexity and still keep the informative value for line scans. The tip is modelled, following the standard ISO 3274, as a spherical tip and two lines, enclosing the apex angle α . The surface profile is integrated as a discretized point cloud with the function $P(x, z=f(x))$ giving the profile height at the coordinate x . To calculate the optimal probing angle of a specific surface point methods and algorithms are required, referred to as a strategy. Several approaches were created and can be categorized in knowledge based, analysing, predicting strategies or a mixture of the aforementioned. A first class of strategies, the knowledge based, uses previous knowledge of the surface profile from an ideal model, e.g. a CAD-file. In the simplest case the tangent for each surface point $P(x, z)$ is calculated with $P_i(x, z)$ being the point number i to be measured and $f_{Stu}(P_i)$ the calculated probing angle:

$$f_{Stu}(P_i) = \frac{\pi}{2} + \tan^{-1} \left(\frac{z_i - z_{i-1}}{x_i - x_{i-1}} \right) \quad (1)$$

A similar class, the analysing strategies, uses the measurement system itself to create a base profile in a first step. In a second step tilting can be applied. This approach does not require previous knowledge and can be applied with unknown profiles. A third class, predicting strategies, calculates the most suited tilt angle by extrapolating already acquired surface points during the measurement. Generally the measurement starts without rotation and the surface points are recorded. The next points are extrapolated based on these values and the applied algorithm. With the estimation of the succeeding profile, the optimal tilt angle is calculated. For this class several extrapolation algorithms were selected and compared. A linear method, a Cubic spline method, a Newtown method, a Lagrange method or an Aitken-Neville method were implemented.

The effectiveness of the strategies and the achievable deviation reduction were compared for different tips and surfaces. Relevant evaluation criteria were e.g. the measurement deviation, the calculated tilt angle or the tilt velocity and acceleration. Different sample surfaces were created to cover usual practical cases.

Figure 2 shows a sphere segment with a diameter of 1 mm, found e.g. on lenses, featuring a continuous change of slope.

The simulated experiment used a tip apex radius of $10 \mu\text{m}$, an opening angle of 60° , a maximal rotation angle of 45° and a linear predicting strategy. At the beginning of the sphere's edge a flank collision occurs and the resulting deviation suddenly rises. With the change of the extrapolated surface slope, a rotation is triggered and the deviation is reduced until it disappears, limited by the rotation speed and the maximum tilt angle. Compared to a regular scan the mean deviation is reduced by 80%.

A second structure features an abrupt transition of 18° between two constant slopes, Figure 3, focussing on the adaption speed. The slope leads to a constant deviation contribution for a non-tilted case without computational probing point compensation. In this scenario predicting strategies completely reduce the deviation and furthermore analysing strategies can initiate the rotation before the slope change occurs. For the latter case the maximum deviation is reduced from $0.51 \mu\text{m}$ without tilt, mainly depending on the tip geometry, to $0.13 \mu\text{m}$ with an analysing strategy. Generally all tested strategies offer a significant deviation reduction and increase the detectable surface slope with a tilting system compared to no countermeasures at all.

3. HARDWARE REALIZATION

To realize the simulated tilting process in a hardware prototype, a controlled precision servo system is necessary to perform the rotation around the tip's working point. A high positioning accuracy with low guidance deviation is essential;

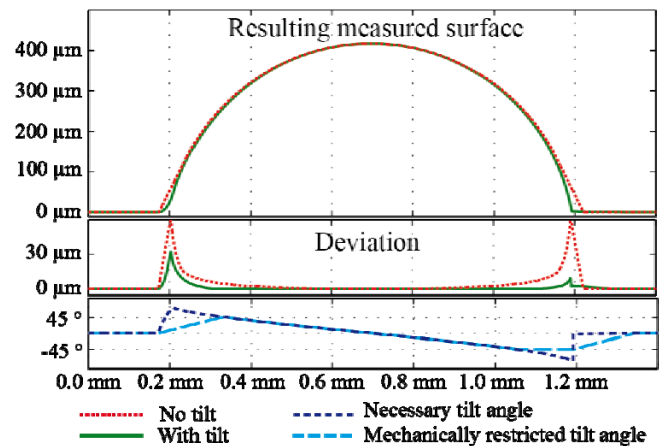


Figure 2. Linear prediction: Sphere segment, 1 mm diameter.

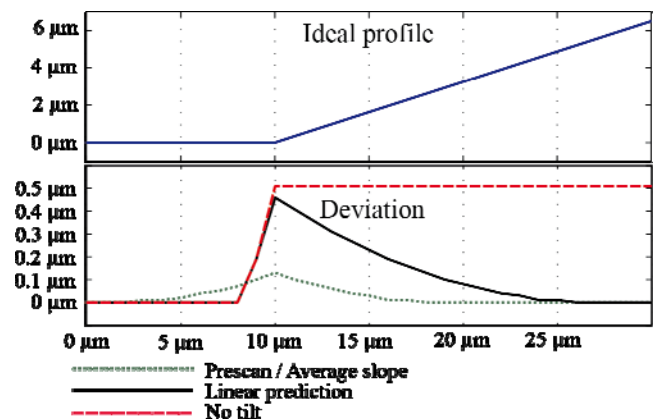


Figure 3. Strategy comparison: 18° ramp profile.

elsewise the measurement deviation would instead be increased when the tip leaves the intended scan trace. The basis of the planned test bed consists of a laser-interferometer controlled nanopositioning and measuring machine type SIOS NMM-1 with an axis resolution of 0.1 nm in three linear axes [11]. In this setup the workpiece is moved by the NMM-1 and the sensor and the rotation unit are installed firmly above. After investigating several kinematic chains, a stacking of two rotary axes was chosen, Figure 4. The axis of the first rotation stage is oriented parallel to the Cartesian height axis of the NMM-1. A second rotary stage under an angle of 45° is mounted below. The second one carries the sensor which is again angled with 45°. In this setup, the centres of both axes align with the working point of the sensor, apart from alignment deviations. The second axis alters the rotation of the sensor, which corresponds to a rotation around the X- and Y-Axis of the NMM-1's Cartesian coordinate system. With the additional movement of the first rotation stage along the Z-Axis the sensor can be adjusted to match any necessary angle around the X- and Y-Axis from -90° to 90° covering a hemisphere.

The importance of angular axis resolution in this setup is reduced by the in-axis alignment of the sensor. The only remaining non-systematic deviation factors are the radial and axial guidance deviations as well as tilt. Positioning window estimations for the selected units result in a maximum deviation of +/- 1.5 µm for the position of the tip. The upper larger axis has a diameter of 100 mm and uses a direct drive. The chosen model features a non-systematic tilt error motion of less than 1 arcsec and a total accuracy of 2 arcsec after calibration by the manufacturer. The lower smaller axis with 30 mm diameter uses a piezoelectric drive with a stick-slip operation for large angles and a scanning operation for small angles and maintaining a position.

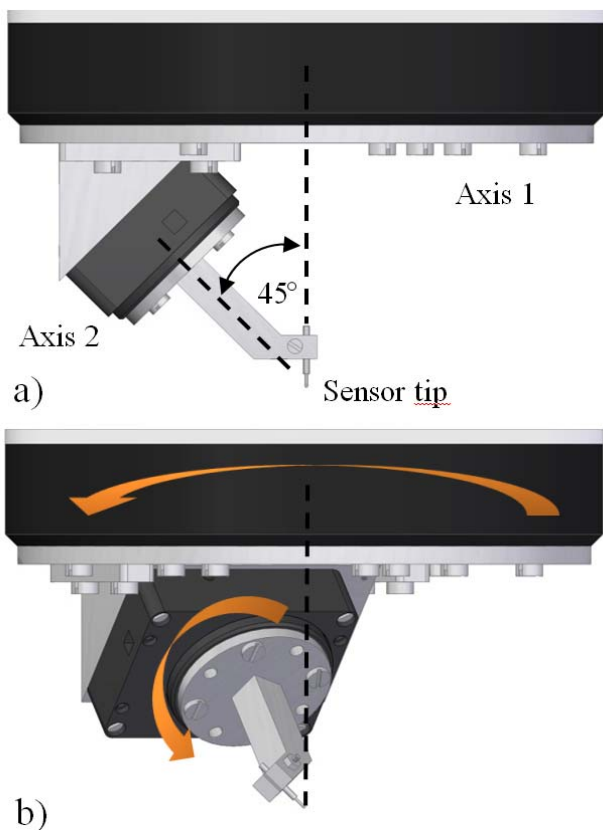


Figure 4. Schematic: a) sensor at 0°; b) sensor at 45°.

Apart from guidance deviations also thermal influence sources and their effects have been respected. To reduce the heat generation in the rotary drives the large axis' control system was fine-tuned to minimize heat generation. Additionally the small piezo stage is self-locking and does not require energy to keep a position. Thermal effects are also respected in the mechanical setup. The 45° connectors between the rotary stages and the sensor are made of Invar, an alloy with a thermal expansion coefficient near zero.

Concerning systematic deviation components the most significant factor is the assembly of the axes and installation of the sensor tip. To support their alignment process, an alignment help was constructively integrated. The tip holder as well as the mounting plate between the axes are designed with a central bore. This way the centre openings of both rotary axes are not obstructed and an uninterrupted optical path to the sensor tip is available. By using a CMM with a video-sensor and a backlight option the centricity of the sensor tip in the axes' centre can be easily assessed. Furthermore the axes' centre bores are used for the wiring of the sensor and the smaller axis. It is refrained from an unlimited number of revolutions to simplify the wiring.

4. REALIZATION OF THE TEST STAND

4.1. Choice of the applied sensor

To accelerate the realization of the prototype a near-tactile probe was selected, equivalent to the simulated deviation mechanics [12], [13]. The working principle of the sensor prototype is derived from scanning tunnelling microscopy (STM) using the current through the nanometre ranged air gap between a conductive tip and workpiece. As opposed to regular STMs no sharp wire tips are used but larger scaled spherical probing tips. The system allows for deliberately shaped tips, ranging from spheres to conical shapes or needles without having to respect mechanical restrictions [13]. For the test stand prototype two tip shapes were chosen. The first scenario uses a hard-metal sphere tip with 0.3 mm diameter equivalent to a tactile probe with a large apex radius. When a probing point at the front of the tip is assumed for reconstruction, the system behaves like a tactile version and the deviation can clearly be shown. The second scenario features a sharp metal needle with a smaller tip angle than a classical profilometer could operate with, equivalent to a near ideal tip.

4.2. Calibration artefact

To calibrate the rotation system an artefact is necessary to determine the position of the sensor probing point in relation to the workpiece coordinate system. With this knowledge theoretically all systematic deviation components from the rotation system including alignment deviations can be compensated. As a reference structure and origin of the workpiece coordinate system a calibrated precision sphere grade G5 with a nominal diameter of 4 mm is used. For the spherical sensor tip, its centre results from the origin of the calibration sphere plus the sum of both radii in probing direction.

As measurement subject three angled planes with rounded transitions are chosen, Figure 5. The angle between each two neighbouring flats is 30°. Additionally all flats are angled in the perpendicular direction too. The test subject is part of a cutting insert separated by wire erosion. With the calibration sphere the position of the rotated sensor can be acquired for all angle steps and the systematic positioning deviations can be compensated.

The resulting correction vectors from the workpiece origin to the probing sphere centre are stored in a calibration field, accessed by the machine control during the scan. Another compensation vector points from the centre of the sensor tip's curvature to its reference contact point. For the used spherical tip this vector compensates for the sphere's radius.

The measurement process with the calibration field is performed in the following steps. Starting at zero rotation a number of points are recorded. The values are transferred from the machine coordinate system into the workpiece coordinate system with the current compensation vectors. Afterwards the algorithms of the chosen strategy are applied, calculating the surface angle and the next suitable tilt angle. For a sufficient large change of angle the probe gets disconnected from the surface and the rotation is performed. An uninterrupted scan without surface disconnection will be realized later. The new probe centre point is loaded from the calibration field and the sensor is brought over the last recorded surface point. Afterwards the measurement continues. An optional fine calibration can be applied to acquire a more recent calibration just after the rotation has been performed.

5. PRELIMINARY TESTS

To implement and test all strategy algorithms and measurement sequences before the setup of the stacked axes was finalized, the test stand was realized with a preliminary rotation unit. A simple manual rotation axis with a diameter of 25 mm was installed to test all algorithms, the strategies and the calibration field. As the manual axis' reproducibility is insufficient and not comparable with the planned automated stages, the described fine-calibration after each rotation was also applied. Figure 6 shows all available data merged in the workpiece coordinate system. Above the hemisphere as the origin are the probe centres from the calibration field at different angles, displayed with a sphere of 0.3 mm diameter. In the shown case, seven angle positions from -30° to 30° were acquired. Due to the used kinematic, the centre points describe a circular path.

A first measurement on the angled flats with the described logic is shown in Figure 7a) and b), split into the left flank and the right flank. The blue curve represents a scan without tilt, assuming a fixed probing point at the lowest part of the tip, as a profilometer would yield. The green curve uses sensor rotation and assumes a moving reference contact vector always aligned in the rotation direction. The rotation is performed with a fixed angular step width of 10° . It can be seen that both ways result in the same values in the flat top, as expected. In the sloped parts the methods differ as the rotated tip is more capable in keeping the actual probing point near the reference point. This can be clearly seen in the beginning of Figure 7a) when the rotated tip starts at 0° and then after some surface points



Figure 5. Calibration sphere and angled flats.

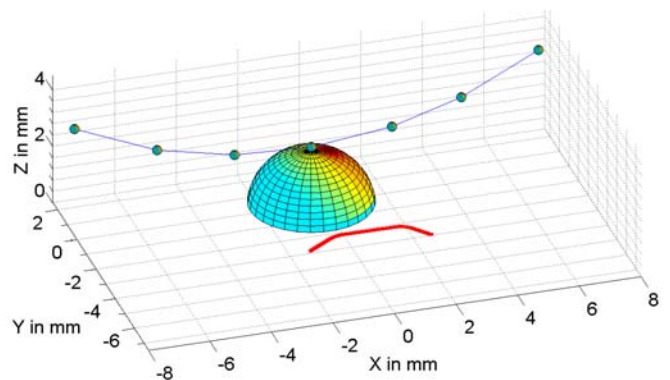


Figure 6. Workpiece coordinate system and all acquired data.

switches to 30° and the deviation is instantaneously reduced. Other effects of interest are discontinuities in the rotated scan. They are caused by the sudden change of the assumed probing vector when the axis is turned with a 10° increment. For the demonstrated test case with the manual axis the measurement deviation was reduced down to $18 \mu\text{m}$.

6. IMPLEMENTATION OF THE STACKED AXES

Parallel to the functional tests with the manual axis the setup and integration of the two stacked rotary axes were performed. This procedure covered the axes' mechanical installation and alignment, the software interface to the axes as well to the NMM-1's control system and the electrical installation of the near-tactile probe.

After manufacturing of the Invar adapter parts, both axes were mounted onto each other and installed overhead in a mounting frame for testing purposes. The control sequences and the corresponding behaviour had to be tested. As both axis controllers can be directly accessed by a C or C++ library, Matlab functions were written to access the library and execute hardware commands. As the NMM-1's host computer uses Matlab for the sequence control the axes can easily be integrated. Command sequences as homing the axes, moving to an angle in the axis coordinate system and retrieving the current angle were realized

The mechanical integration into the NMM-1 was realized

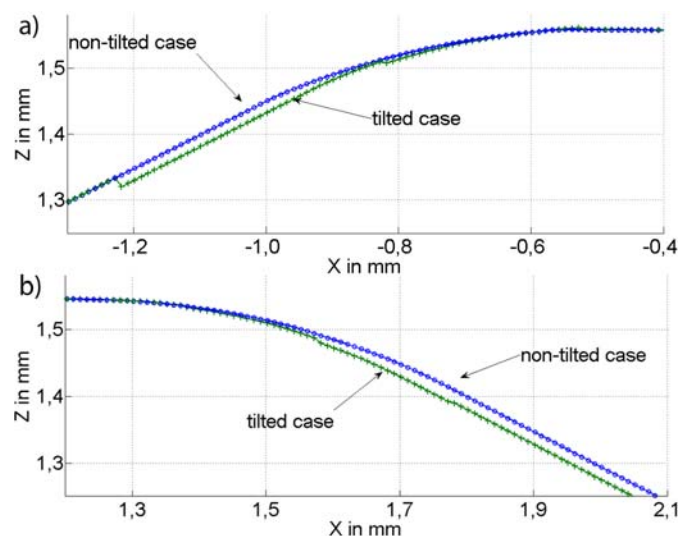


Figure 7. Angled flat: a) Left transition; b) Right transition.

with a regular plug-in module for sensor exchanges in the NMM-1. For this purpose the NMM-1's top plate, as part of the metrological frame, has a slot for a plug-in module. The plug-in plate was also made of Invar and carries the rotary axes below it. To have sufficient clear space below the top plate, its mounting height was increased by 76 mm by adding Invar distance sleeves. The sleeves and the plug-in served to position the sensor tip in the virtual crossing of all laser beams of the NMM-1. This way the Abbe-principle for the NMM-1's axes is fulfilled [14]. During the design the collision volumes of the rotation axes and the NMM-1's workpiece carrier were relevant as the edge of the corner mirror is higher than the workpiece mounting plane. By safe construction the movement volumes don't overlap at any position or rotation angle and an involuntary collision is avoided. Figure 8 shows the installed axes in the NMM-1. The workpiece carrier and the border of the laser reflectors are located under a white protective casing.

For the integration of the sensor an electrical connection between the tip holder and the workpiece was necessary. The tip holder is mounted on the small rotary axis which top plate is electrically isolated. The tip holder is connected to a precision voltage source to set the tip under operating voltage. The workpiece carrier is electrically connected to protective earth, therefore an additional isolation layer was installed. The workpiece is mounted on the carrier plate as already shown in Figure 5. The carrier plate is electrically connected by a flexible shielded wire to an amplifier circuit. It converts during operation the current in the nanoampere range to a corresponding voltage in the volt range. This sensor signal is connected to the input port of the NMM-1.

On the software side the sensor is integrated by configuring the input ports and recording a sensor characteristic. By storing a third order polynomial in the digital signal processor of the NMM-1 the momentary displacement between sensor and workpiece to a chosen setpoint can be calculated and used for position control during a surface scan. Another possible way of operation is the recording of only a single surface point after the setpoint is reached, similar to a touch-trigger probe.

With the integration of the stacked axes all steps performed with the manual axis were repeated. First the calibration field was recorded again with angle increments from -30° to $+30^\circ$ in 5° steps in the XZ-Plane of the NMM-1. In comparison to the manual axis an additional coordinate translation step had to be added to find the corresponding angles of each stacked rotary axis for a given angle in the NMM-1's Cartesian coordinate system. For simplification this nonlinear relationship was calculated beforehand and stored in a lookup table.



Figure 8. Axis setup installed in the NMM-1.

7. AUTOMATED SENSOR TILTING

After implementation of all necessary command sequences an automated measurement on the angled flats was repeated. The angled flats measurement was started again at no rotation and after enough recorded values the surface angle was determined to be -30° . The tip was removed from the surface and rotated by -30° along the Y-axis perpendicular to the scan-line. With the knowledge of the tip centre position in the workpiece coordinate system the contact point from the last measurement point was determined and re-addressed with the rotated tip. Figure 9 shows the system during operation on the cutting insert.

The results are displayed in Figure 10 showing the first half of a 3 mm line scan. Again the blue curve uses a fixed reference contact point like a regular profilometer, the green curve uses the sensor rotation principle and keeps the tip rectangular to the surface. The deviation is again reduced to $18\ \mu\text{m}$ with the large 0.3 mm tip.

With the sensor rotation prototype just completed and the first results of an automated measurement process acquired, further aspects can be investigated. The next steps cover the determination of the achievable repeatability of the setup and the measurement on other calibrated artefacts like e.g. a micro-contour artefact.

8. CONCLUSIONS

A probing principle based on dynamic sensor tilting is investigated with a rotation around the sensor's working point. The measurement deviation mechanics and strategies to deliver optimal rotation angles are modelled in a simulation environment. The results demonstrate the improvement by sensor tilting on practical test samples, reducing measurement deviation and increasing the usable surface slope. The principle was transferred to a hardware prototype based on a nanopositioning and measuring machine with an axis resolution of 0.1 nm as test stand. The kinematic chain for the sensor rotation consists of two stacked rotary axes under an angle of 45° allowing two rotary degrees of freedom. Occurring error sources like thermal effects are minimized by the stringent use of materials with low thermal expansion coefficients. To reduce the remaining systematic positioning deviation of the rotation unit an in-situ calibration strategy was realized and applied. The test stand has been completed and a mechanical, electrical and software-side integration was performed. As sensor a proven near-tactile electrical sensor type was applied to accelerate the setup and allows for a wider range of sensor tips. First results of

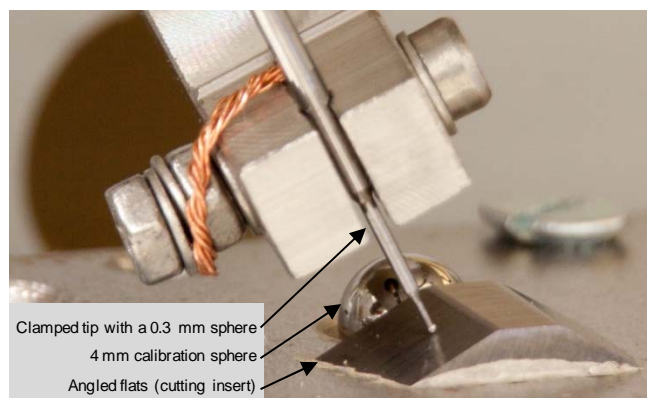


Figure 9. Tilted measurement process.

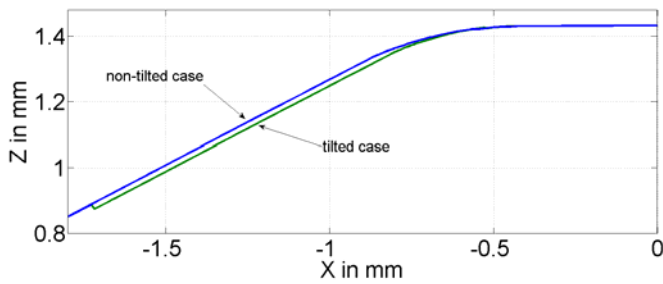


Figure 10. Cutting insert measurement with the final setup.

the automated sensor tilting were gathered on a cutting insert with a surface angle range from -30° to $+30^\circ$. The increase of the possible operation angle and the measurement deviation reduction is demonstrated. Future tasks cover the assessment of the repeatability of the rotary sensor positioning and measurements on different calibrated sample surfaces in comparison with regular profilometers.

ACKNOWLEDGEMENT

This article is based on the research project “Ultra-accurate acquisition of highly curved surfaces by slope-dependant dynamic sensor tracking with rotatory flexure hinges”. The authors thank the German Research Foundation (Deutsche Forschungsgemeinschaft, DFG) for supporting this research.

REFERENCES

- [1] M. Krystek, ISO filters for precision engineering, *Technisches Messen* 76 (2009) pp. 133-159.
- [2] P.M. Lonardo, H. Trumpold, L. De Chiffre, Progress in 3D surface microtopography characterization, *Annals of the CIRP* 45 (1996) pp. 589-598.
- [3] A. Weckenmann, T. Estler, G. Peggs, D. Mcmurtry, Probing systems in dimensional metrology, *Annals of the CIRP* 53 (2004) pp. 657-84.
- [4] D. Keller, Reconstruction of STM and AFM images distorted by finite-sized tips, *Surface Science* 253 (1991) pp. 353-364.
- [5] H.N. Hansen, K. Carneiro, H. Haitjema, L. De Chiffre, Dimensional micro and nanometrology, *Annals of the CIRP* 55 (2006) pp. 721-743.
- [6] E. Lebrasseur, J.-B. Pourciel, T. Bourouina, T. Masuzawa, H. Fujita, A new characterization tool for vertical profile measurement of high-aspect-ratio microstructures, *Journal of Micromechanics and Microengineering* 12 (2002) pp. 280-285.
- [7] Y. Hua, C. Coggins, S. Park, “Advanced 3D metrology Atomic Force Microscope”, *Proceedings ASMC 2010*, July 11-13, 2010, San Francisco, USA, pp. 7-10.
- [8] F. Marinello, P. Bariani, A. Pasquini, L. De Chiffre, M. Bossard, G.B. Picotto, Increase of maximum detectable slope with optical profilers, through controlled tilting and image processing, *Measurement Science and Technology* 18 (2007) pp. 384-389.
- [9] A. Weckenmann, X. Jiang, K.-D. Sommer, U. Neuschaefer-Rube, J. Seewig, L. Shaw, T. Estler, Multisensor data fusion in dimensional metrology, *Annals of the CIRP* 58 (2009) pp.701-721.
- [10] A. Weckenmann, A. Schuler, R.J.B. Ngassam, “Enhanced measurement of steep surfaces by sensor tilting”, *Proceedings of the 56th international scientific colloquium*, Sept. 12-16, Ilmenau, Germany, 2011, ID 134:1.
- [11] E. Manske, T. Hausotte, R. Mastlylo, T. Machleidt, K.-H. Franke, G. Jäger, New applications of the nanopositioning and nanomeasuring machine by using advanced tactile and non-tactile probes, *Measurement Science and Technology* 18 (2007) pp. 520-527.
- [12] A. Weckenmann, J. Hoffmann, “Long range 3D scanning tunnelling microscopy”, *Annals of the CIRP* 56 (2007) pp. 525-528.
- [13] J. Hoffmann, A. Schuler, Nanometer resolving coordinate metrology using electrical probing, *Technisches Messen* 78 (2011) pp. 142-149.
- [14] I. Schmidt, T. Hausotte, U. Gerhardt, E. Manske, G. Jäger, Investigations and calculations into decreasing the uncertainty of a nanopositioning and nanomeasuring machine (NPM-Machine), *Measurement Science and Technology* 18 (2007) pp. 482-486.